

## Threshold wind velocity for snow drifting as a function of terminal fall velocity of snow particles

Kengo SATOH, Shuhei TAKAHASHI

Kitami Institute of Technology, Kitami 090–8507, Japan

(Received September 1, 2005; Revised manuscript accepted November 16, 2005)

### Abstract

The threshold wind velocity  $V_T$  for snow drifting depends on the snow particle shape and its surface condition. To explain the effect of particle shape on  $V_T$ , we employ the terminal fall velocity of snow particles, which, similar to  $V_T$ , depends on the aero resistance coefficient. For snow samples obtained from a natural snow surface,  $V_T$  was measured by a wind tunnel experiment, and the terminal wind velocity  $w$  was measured in a cylinder. In addition, the repose angle was also observed. For estimating the friction between the particles,  $V_T$  and  $w$  were considered to be dependent on particle shape. For a dendrite crystal,  $V_T$  and  $w$  were determined to be 3–7 m/s and 0.4–0.9 m/s, respectively; further,  $V_T$  tended to be proportional to  $w$ . The  $V_T/w$  ratio of other particles was larger than that of the dendrite crystals; this is explained by the existence of a bonding force.

### 1. Introduction

In Antarctica, snow drifting is an important factor in the estimation of the surface mass balance of an ice sheet. Budd *et al.* (1966) estimated the snow drift transport rate based on observations of the snow drift flux. Radok (1977) discussed a vertical profile of drift density by the diffusion theory of drifting snow (Shiotani and Arai, 1953), in which the terminal fall velocity of the snow particles is important. Takeuchi *et al.* (1975) compiled the threshold wind velocity  $V_T$  for drifting snow, which is the wind speed at which snow particles begin to move.  $V_T$  varied with air temperature: 8–10 m/s near 0°C and 4–5 m/s below –5°C. It also depended on the snow particle shape or the aerodynamic characteristics of the snow particles. The terminal fall velocity  $w$  depends on dynamic characteristics in a similar manner as  $V_T$ , and  $w$  can function as an indicator of  $V_T$ , although there are limited observations of  $w$  for drifting snow particles (Takahashi, 1985). In our study,  $V_T$  was measured in a small wind tunnel for snow samples obtained from a natural snow surface, and  $w$  was observed by simulating snowfall with the sampled snow particles. In addition, the adhesive force of the snow particles was measured by a repose angle observation.

### 2. Principles of the observations

The movement of a snow particle is initiated when the drag force  $F_V$  exerted by the wind exceeds the horizontal resistance  $F_s$  (Fig. 1). The horizontal resistance  $F_s$  consists of the friction force  $F_f$  and the bonding force between the particle and snow surface  $F_b$  which is the maximum force for bond breaking (Fig. 2a). The force  $F_v$  acting on a snow particle can be expressed as follows:

$$F_V = \frac{1}{2} C \rho_a S V^2, \quad (1)$$

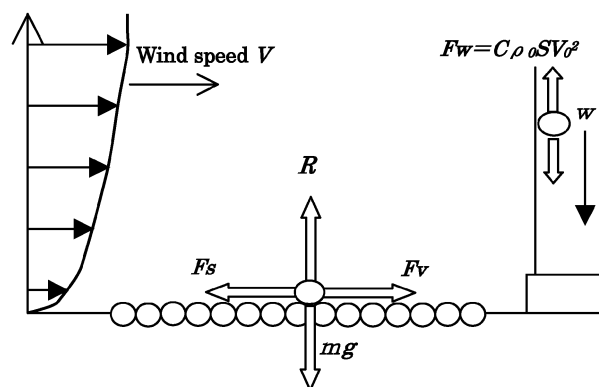


Fig. 1 Representation of force acting on snow particles in terms of threshold wind velocity and terminal fall velocity.

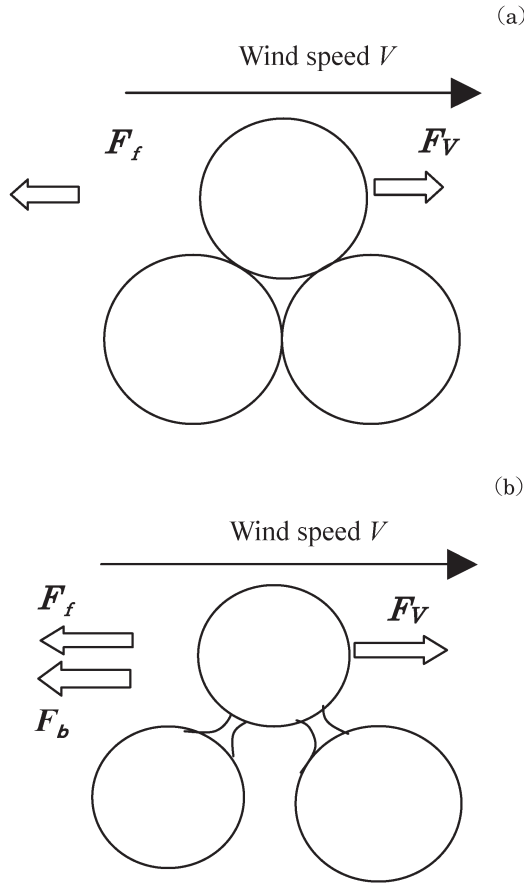


Fig. 2 Horizontal components of forces acting on a particle. (a)  $F_v$  is the drag force exerted by the wind, and  $F_f$  and  $F_b$  are the friction force and bonding force, respectively. (b) Horizontal components of forces excluding  $F_b$ .

where  $C$  is an aero resistance coefficient;  $\rho_0$ , the air density;  $S$ , the cross sectional area of the particle; and  $V_0$ , the wind velocity at the height of the snow particle radius. The horizontal resistance  $F_s$  is the sum of the friction force  $F_f$ , which is not an actual friction force but can be expressed as  $F_f = \mu mg$  since it depends on  $mg$ , and the bonding force  $F_b$ :

$$F_s = \mu mg + F_b, \quad (2)$$

where  $\mu$  is a friction coefficient (static);  $m$ , the mass of the snow particle;  $g$ , the acceleration due to gravity; and  $F_b$ , the bonding force (the maximum force for bond breaking). When a snow particle begins to move,  $F_v$  and  $F_s$  are balanced, and the following relation is deduced:

$$\frac{1}{2} C \rho_0 S V_0^2 = \mu mg + F_b. \quad (3)$$

In order to analyze the aero resistance coefficient  $C$ , we employ  $w$  of a snow particle, which is dependent on  $C$  and is measurable. Since the air resistance balances the force of gravity in still air, often decreasing with sufficient distance, the air drag force also balances the force of gravity, and

$$\frac{1}{2} C \rho_0 S w^2 = mg, \quad (4)$$

from which

$$w = \sqrt{\frac{2mg}{C \rho_0 S}}. \quad (5)$$

If a particle is assumed to be a sphere of diameter  $d$  with density  $\rho$ , Eq. 5 is modified as

$$w = \sqrt{\frac{4\rho g d}{3C \rho_0}}, \quad (6)$$

where  $w$  is a function of the root of the diameter  $d$  for a constant  $\rho$ . Though  $V_0$  in Eq. 1 is the wind velocity at the height of the particle radius,  $V_T$  was measured over the surface at the center of the wind tunnel. In this case,  $V_T$  is proportional to  $V_0$  at the anemometer height;

$$V_T = K V_0. \quad (7)$$

Assuming a logarithmic vertical distribution of wind velocity,  $K$  is represented by the surface roughness  $Z_0$ , the particle radius  $Z_1$  and the anemometer height  $Z_2$ ;  $K = \ln(Z_2/Z_0)/\ln(Z_1/Z_0)$ . When  $Z_0$  is 0.05 mm,  $Z_1 = 0.5$  mm and  $Z_2 = 25$  mm (centre of wind tunnel section),  $K = 2.7$ .

If we apply this relation to natural wind for the normal anemometer height of 1.5 m to 5.0 m,  $K$  acquires a value between 4.5 and 5.0. Using Eqs. 3, 4 and 7,  $V_T$  is derived as

$$V_T = K \sqrt{\frac{2(\mu mg + F_b)}{C \rho_0 S}}. \quad (8)$$

Since it is difficult to measure the aero resistance coefficient  $C$  in Eq. 8,  $V_T$  is represented as a function of  $w$  by using Eq. 4;

$$V_T = K \sqrt{\mu + \frac{F_b}{mg}} \cdot w. \quad (9)$$

If  $F_b$  in Eq. 9 is considered to be negligible, as shown in Fig. 2b,  $V_T$  is reduced to

$$V_T = K \sqrt{\mu} \cdot w. \quad (10)$$

Thus,  $V_T$  is principally proportional to  $w$ , as shown in Eq. 9. If we can measure the friction coefficient  $\mu$ , the bonding force  $F_b$  per mass of the particle can be obtained from Eq. 9.

### 3. Observation method

The observations of  $V_T$  and  $w$  were performed daily between 7 and 9 a.m. from 1 January to 28 February 2003 at the athletics field of the Kitami Institute of Technology, Kitami, Hokkaido. The observation methods were almost identical to those of Satoh *et al.* (2003). In order to measure  $V_T$ , a small

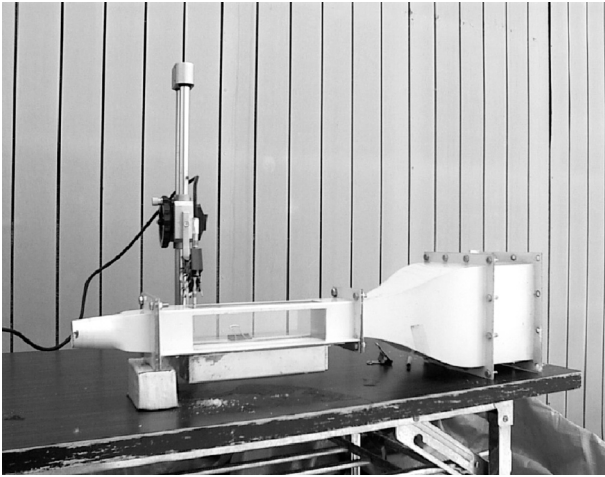


Fig. 3 Small wind tunnel used in the measurement of threshold wind velocity. Working section; width: 50 mm, height: 50 mm and length: 200 mm. A particle was procured from a natural snow surface without disturbing it and was placed at the bottom of the wind tunnel.

wind tunnel (working section; length: 200 mm, width: 50 mm and height: 50 mm) was used outdoors (Fig. 3). The snow sample (length: 200 mm, width: 50 mm, and depth: 20 mm) was transferred from a natural snow surface using a case, so as not to disturb it and was placed at the bottom of the wind tunnel. The wind speed in the wind tunnel was gradually increased, and  $V_T$  was measured as the wind speed at which the snow particles began to move. Wind speed measurements were carried out at 25 mm high, leeward end of the wind tunnel, with a thermal thermistor anemometer. The experiment was repeated five times and the average of  $V_T$  was used for the calculations.

The velocity of falling snow and snow particle size were measured in a cylinder having a diameter of 8 cm and height of 180 cm by using two infrared ray sensors (Fig. 4).

The two sensors were positioned 20 mm apart inside a box below the cylinder, and they measured the time taken by a particle to traverse the two infrared rays (lapse time). The terminal velocity was obtained from the lapse time, and the snow particle size was obtained from the reduction in infrared ray intensity. The upper sensor was employed for data logging, while the lower sensor was used to measure particle size. Because the lower sensor was wider than the upper one, the ‘edge effect’, an error in particle size measurement, which occurs when a particle passes at the edge of an infrared ray, was avoided. In our system, the cross section of the infrared ray beam used in the upper sensor was 4 mm and 1 mm in width and thickness, respectively, while that of the beam in the lower sensor was 10 mm and 1 mm in width and thickness, respectively.

In every observation, the photomicrograph of the



Fig. 4 System for terminal fall velocity measurement. Particles were allowed to fall in a cylinder. Their speed and size were measured when they passed through the two infrared rays of the sensors.

snow particle was taken in a cold room and the particle shape was distinguished.

## 4. Results

### 4.1 Threshold wind velocity

Observations for  $V_T$ ,  $w$  and repose angle ( $\theta$ ) were conducted every morning between 1 January and 28 February 2003. In Fig. 5,  $V_T$  and metrological conditions are shown. The time of the observations are indicated by snow particle-shaped symbols on the air temperature trend. Temperatures during the observations were  $-0.8^\circ\text{C}$  to  $-21.6^\circ\text{C}$ , while the air temperature was between  $-24.4^\circ\text{C}$  and  $3.0^\circ\text{C}$ .

In Fig. 5, we suppose that  $V_T$  is dependent on particle shape and elapsed time after snowfall.  $V_T$  was 3–6 m/s for the dendrite crystals indicated as \* in Fig. 6 and 5–12 m/s for the broad branches indicated as  $\diamond$ . In the case of dendrite crystals with rime, indicated as  $\circ$ ,  $V_T$  was 6–13 m/s. These values—larger than those for dendrite—indicate that the snow particles become heavier by riming, and the value of  $V_T$  depends on the amount of rime.

After snowfall,  $V_T$  increased to 10–15 m/s in a short period of 1 to 3 days. When the snow particles experienced melting and refrozen (melting metamorphism),  $V_T$  reached 15 m/s, which is the wind speed limit for wind tunnel system. A similar variation was observed in  $w$ ; however, variation was not so large as  $V_T$ .

In order to apply the value of  $V_T$  obtained from wind tunnel experiments to the usual anemometer

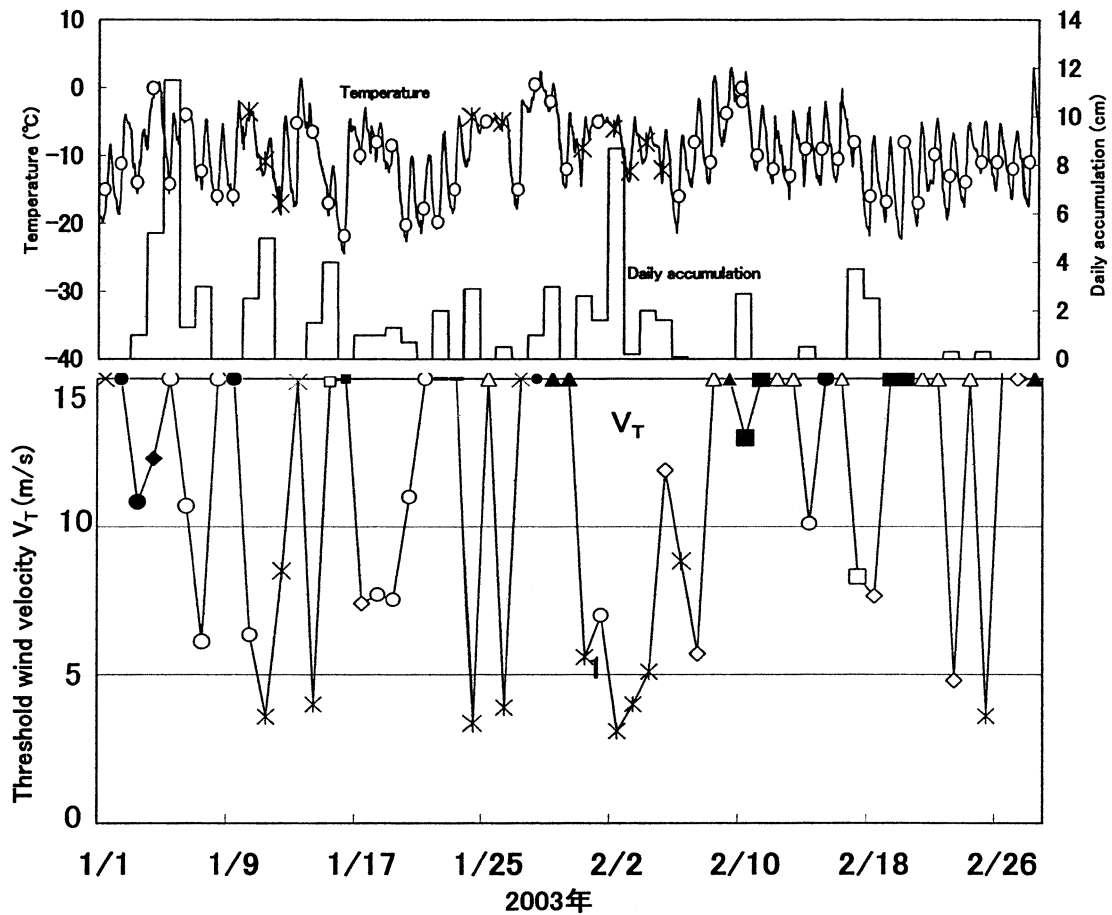


Fig. 5 Threshold wind velocity, daily snowfall depth and temperature from 1 January to 28 February 2003, where  $C$  is 1. The symbols used are as follows: \* represents the dendrite crystals;  $\times$ , melting dendrite crystals;  $\circ$ , dendrite crystals with rime;  $\bullet$ , melting dendrite crystals with rime;  $\diamond$ , broad branches;  $\blacklozenge$ , melting broad branches;  $\square$ , broad branches with rime;  $\blacksquare$ , melting broad branches with rime;  $\triangle$ , surface hoar;  $+$ , needles;  $\blacktriangle$ , granular particles. In the name of particle shape, "melting" (shown by solid symbols) is for the particles, which experienced melting metamorphism, although they were usually refrozen at measurement time.

heights in experiments conducted in natural wind,  $V_T$  should be multiplied by 1.6 and 1.9 for anemometer heights of 1.5 m and 5 m, respectively. However, the turbulence encountered in natural wind tends to cause snow drifting at a small average wind speed. These opposite factors compensate each other; therefore,  $V_T$  in a wind tunnel is close to that in natural wind. The minimum value of  $V_T$  for a dendrite crystal in the wind tunnel experiment was around 3 m/s and that in natural wind is around 4 m/s; their ratio is approximately 1.3. Therefore,  $V_T$  obtained from wind tunnel measurements can be applied to natural drifting snow by using a multiplication factor of around 1.3.

#### 4.2 Terminal fall velocity

The relation between  $w$  and particle size are shown in Fig. 6. The data of around 100 particles were averaged for daily experiments. The lines in Fig. 6 are based on the relation expressed in Eq. 6, with different particle densities.  $C$  is about 0.5 for a sphere and 1.0 for disc under  $10^4$  of  $Re$  (Reynolds number), whereas it

may be larger than 1.0 for a dendrite crystal due to its complicated shape, and close to 0.5 for round shape particle.  $C$  for lines in Fig. 6 was assumed to be 1 for a disc.  $w$  of the dendrite crystals was primarily 0.5–0.8 m/s, which is located below an equidensity line of around  $25 \text{ kg/m}^3$ . In the case of the dendrite crystals with rime, the range of  $w$  was 0.6–1.1 m/s, which were distributed on the  $50\text{--}100 \text{ kg/m}^3$  lines. For the melting particles, the range of  $w$  was 0.6–1.3 m/s, which were distributed between the  $100\text{--}200 \text{ kg/m}^3$  lines. The large  $w$  values of the melting particles were due to their large density, which resulted from their spherical shape. In other words, in the case that a snow particle melts with maintaining a mass constant, the area of cross section  $S$  in Eq. 5 decreases with decreasing diameter, and  $w$  increases with an increase in density  $\rho$ , according to Eq. 5.

The relation between  $V_T$  and  $w$  is shown in Fig. 7. The variation in  $V_T$  was larger than that in  $w$  for the entire data. For the dendrite crystal, the range of  $V_T$  was 3–7 m/s and that of  $w$  was 0.4–0.9 m/s, and  $V_T$  tended to be proportional to  $w$ . In this case, the ratio of

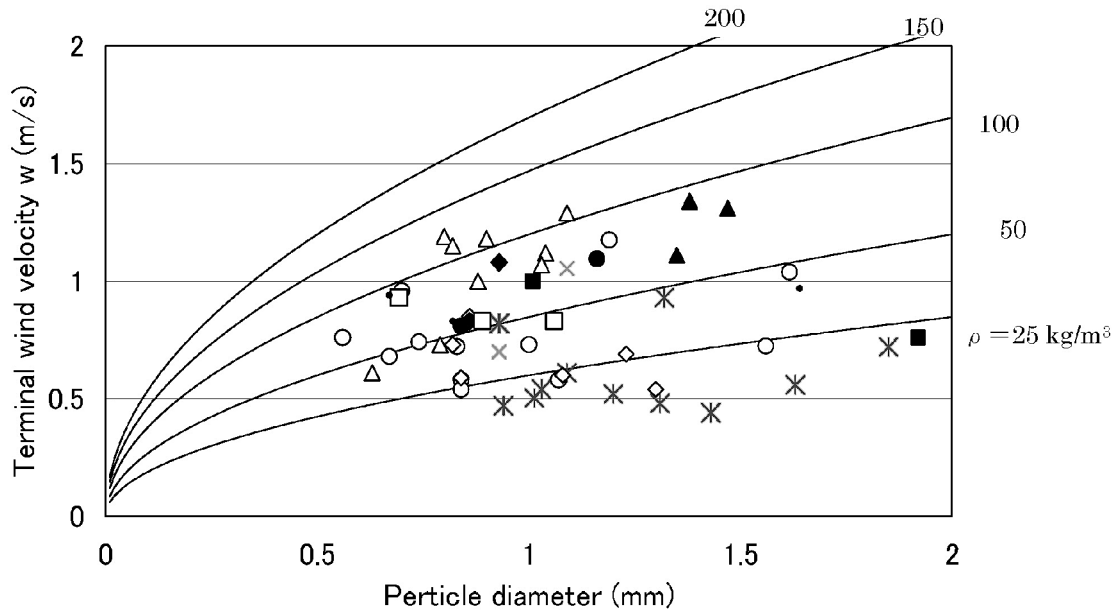


Fig. 6 Relation between terminal fall velocity and particle size. Curved lines of equal density are derived from Eq.6. Symbols are the same as in Fig. 5.

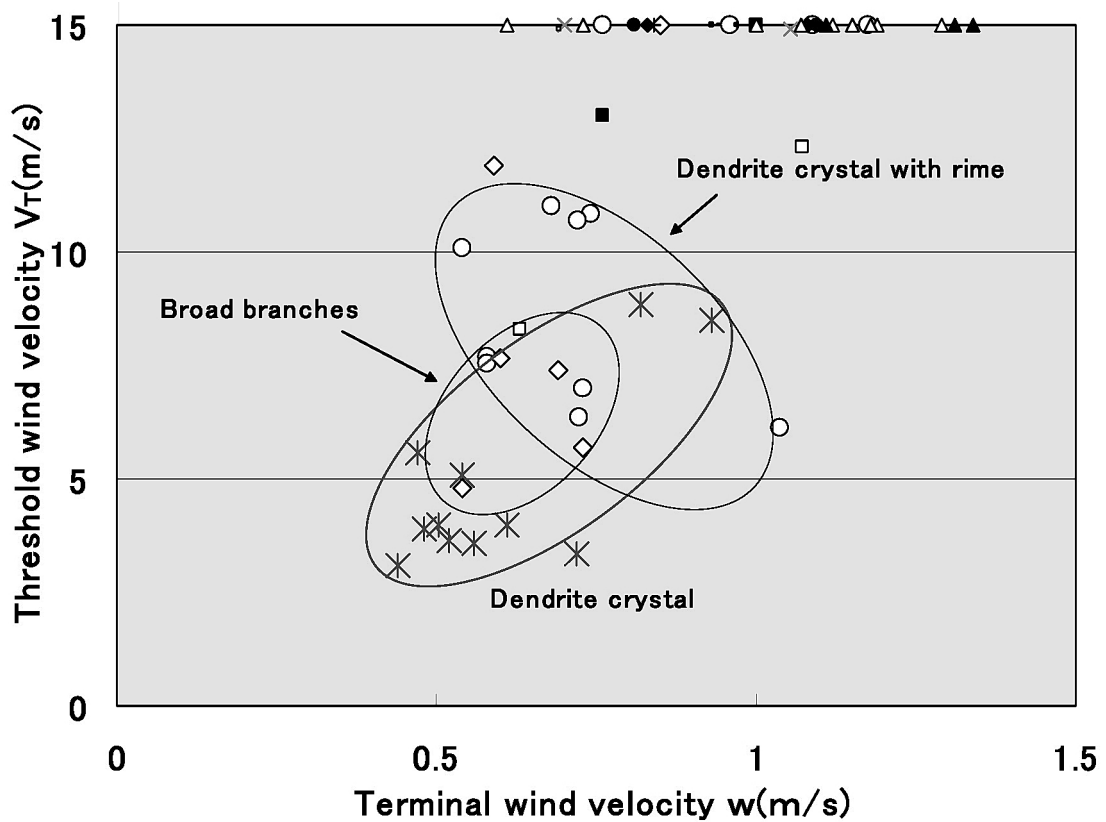


Fig. 7 Threshold wind velocity  $V_T$  and terminal fall velocity  $w$ . Symbols are the same as in Fig. 5.

$V_T/w$  was around 7-10; this can be explained by using the friction coefficient in Eq. 10. For the dendrite crystal with rime,  $V_T$  was 5-12 m/s and  $w$  was 0.5-1.0 m/s. In their relation is more scatter and larger than the proportional relation for dendrite crystals. Since the effect of mass increase by rimes is same for  $V_T$  and  $w$ , one of the causes of large scattering  $V_T$  is relatively

large cohesion due to high temperature when it fell. For the broad branch,  $V_T$  was 6-15 m/s and  $w$  was 0.6-0.8 m/s. For surface hoar, granular particles and other melting particles, the  $V_T$  values exceeded the measurement limit of 15 m/s. The  $V_T/w$  ratios of these particles were larger than those of the dendrite crystals. This large ratio is probably due to the existence

of the bonding force, as expressed in Eq. 9.

4.3 *Repose angle*

In order to examine the friction coefficient  $\mu$  in Eq. 10, the repose angle, which is the maximum slope angle created when snow particles pile up, was observed. In order to measure the repose angle, the snow particles sampled from a natural snow surface were allowed to fall and accumulate on a disk of diameter 6 cm placed in a box (Fig. 8). The accumulated snow forms a cone, and its slope angle was measured as the repose angle. The friction coefficient  $\mu$  is given as

$$\mu = \tan\theta. \tag{11}$$

The relation between the repose angle  $\theta$  and threshold wind velocity  $V_T$  is shown in Fig. 9, where the  $\mu$  values are plotted on the upper axis. The curves in the figure are lines of equal values of  $w$  derived from Eq. 10. The dendrite crystals exhibited  $\theta$  values of 80–90°, which were mostly on or below the  $w=0.5$  m/s line. For the melting particles,  $\theta$  was measured as 25–50° ( $\mu=0.5$ –1.2) and  $V_T$  was 15 m/s (limit of the measurement), which were largely beyond the lines of their  $w$  values ( $w=1$ –2 m/s). The large deviation from the lines of  $w$  for the melting particles was due to the existence of the bonding force  $F_b$  shown in Eq. 9.

4.4 *Bonding force*

The bonding force  $F_b$  is deduced from Eq. 9

$$\frac{F_b}{mg} = \frac{V_T^2}{K^2 w^2} - \mu. \tag{12}$$

Since it is difficult to separate  $F_b$  and the gravity force  $mg$ , the  $F_b/mg$  ratio was obtained by substituting  $V_T$  and  $w$  in Eq. 12.  $F_b/mg$  is a ratio of the bonding force of a particle to its gravity force; and we refer to it as ‘normalized bonding force’ in this study. From the observed  $V_T$ ,  $w$  and  $\mu$  values, this normalized bonding force is evaluated by using Eq. 12. For the dendrite crystals in the evaluation, the  $\mu$  values were

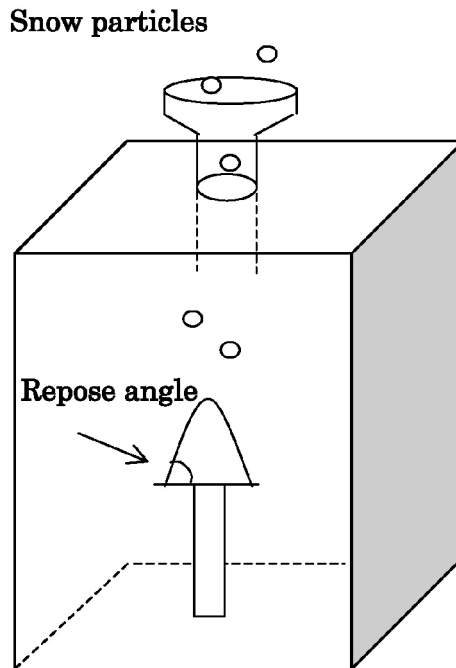


Fig.8 Outline of repose angle measurement. Snow particles were allowed to fall on a disk, and the slope angle of the cone was measured.

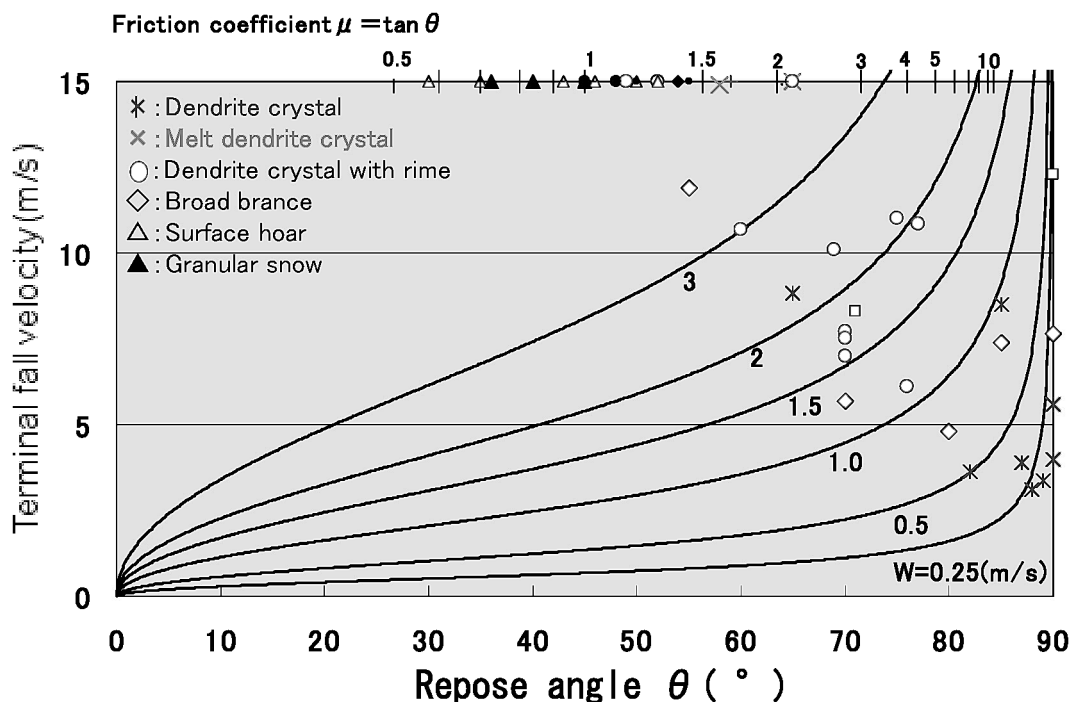


Fig. 9 Relation of repose angle  $\theta$  to threshold wind velocity. Friction coefficient is plotted on the upper axis. Curves are lines of equal value of terminal fall velocity  $w$ . Symbols are the same as in Fig. 5.

limited to 10 because the accuracy of a repose angle is not high enough when it exceeds 85°. For melting particles with a  $V_T$  of 15 m/s, i.e. the limit of the wind tunnel experiment, the  $V_T/w$  ratio was assumed to be approximately 20; this was estimated from melting particles with  $w$  and  $V_T$  values of 0.6 m/s and 15 m/s, respectively. The variation in  $F_b/mg$  for the year 2003 is shown in Fig. 10.  $F_b/mg$  of new precipitation was smaller than 20; especially that of dendrite crystals was usually almost 0. After snowfall,  $F_b/mg$  increased and reached 50 (a limit of measurement) in one or two days.

Fig. 11 shows the relation between  $F_b/mg$  and  $w$ . For the dendrite crystals,  $F_b/mg$  was negligible, except for two cases in which surface hoar or crystals with rime was slightly mixed. The range of  $F_b/mg$  was 0–50 for the dendrite crystals with rime and 5–10 for the

broad branches. For the melting particles,  $F_b/mg$  was large—greater than 50.

Though it is difficult to measure  $F_b$  and  $mg$  separately,  $F_b$  can be estimated as  $1.5\text{--}2.5 \times 10^{-4}$  (N) for a precipitation equivalent to 1 mm-diameter ice sphere.

### 5. Discussion

Variation of  $V_T$  and  $w$  is considered as follows. When  $F_b$  is negligible small,  $V_T$  is proportional to  $w$  as Eq. 10. In this case, when diameter and mass changed with particle metamorphism,  $V_T$  and  $w$  vary in the same proportional relation. When  $F_b$  became large without change of  $w$ , the proportional coefficient will increase large as Eq. 9. This concept is shown in Fig. 12, in which two thick arrows show these two types of variation. In the natural condition, these variations

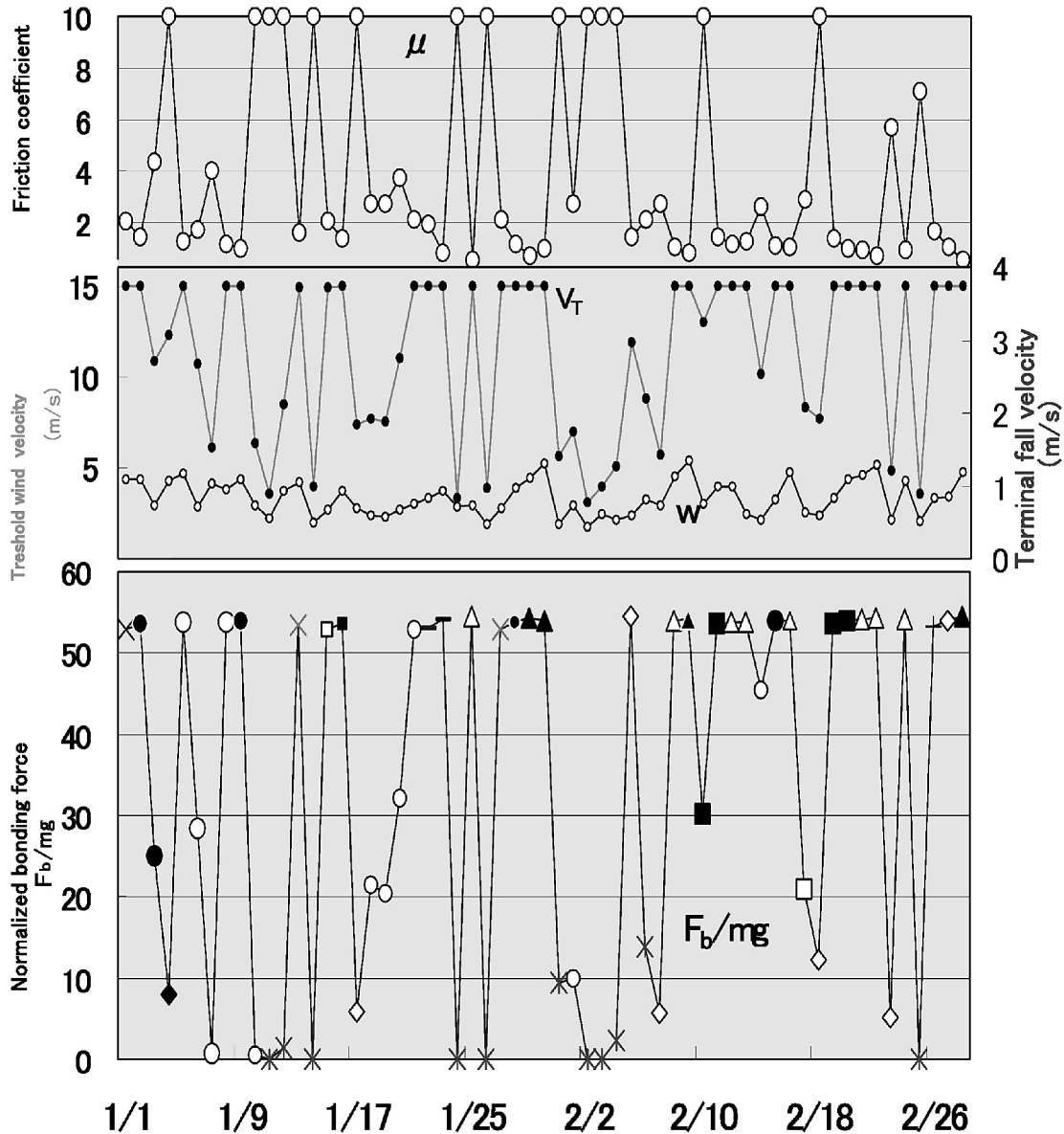


Fig. 10 Variation of normalized force  $F_b/mg$ , threshold wind velocity  $V_T$  and friction coefficient  $\mu$  for January and February 2003. Symbols on the  $F_b/mg$  line are the same as in Fig. 5

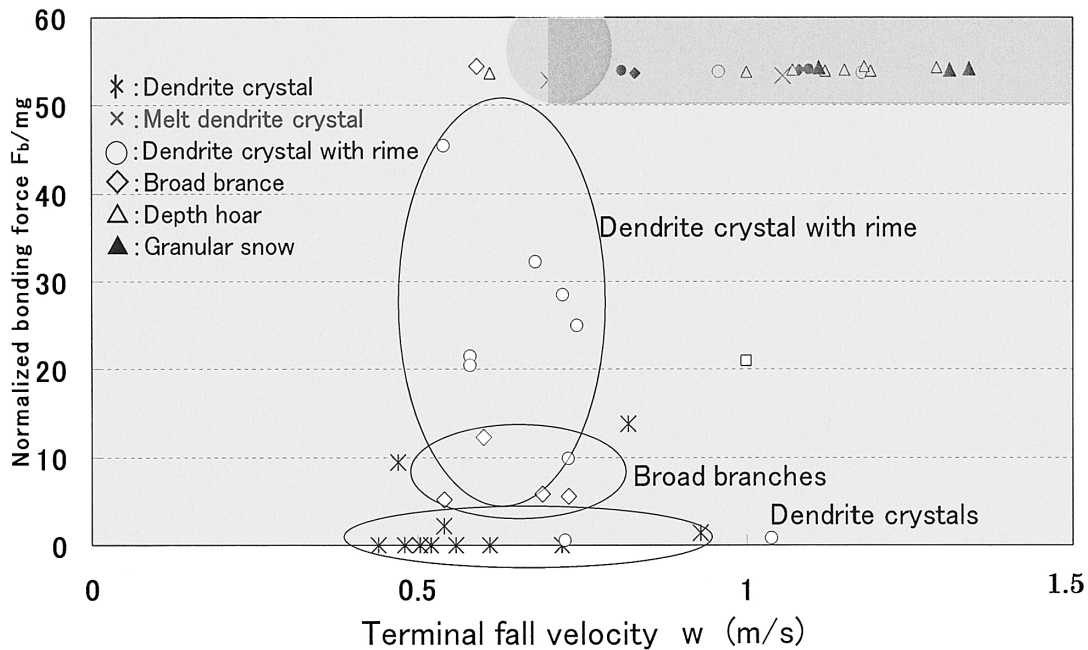


Fig. 11 Normalized bonding force  $F_b$  and terminal fall velocity  $w$ . Symbols are the same as in Fig. 5

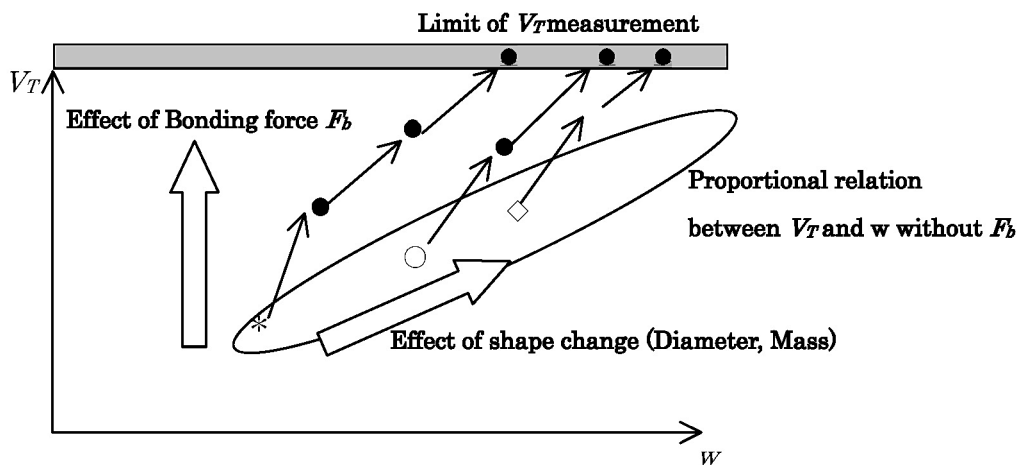


Fig. 12 Concept of variation of  $V_T$  and  $w$  was shown. Two thick arrows show these two types of variations bonding force and shape change. This arrow shows combination of these variations for particles after snowfall.

occur simultaneously as shown by thin arrows in Fig. 12. In our measurement, after snowfall  $V_T$  and  $w$  become large day-by-day, in which especially  $V_T$  increased rapidly and reached to the measurement limit (15 m/s) in 2 or 3 days. The data distribution of Fig. 7 shows that the dendrite crystal and broad branches are on a same proportional relation, but dendrite crystal with rime scattered largely. This deviation would be caused by existence of  $F_b$  adding to larger cohesion under high temperature as described in 4.2. Though the reason of this large  $F_b$  cannot be specified, one of speculation is that dendrite crystals with much rimes are heavier and tend to catch snow surface like an anchor, and another one is that air temperature, when this crystals fall, was relatively high and bonds grow

rapidly.

In Eq. 9, which shows the relation between  $V_T$  and  $w$ , contains  $F_b/mg$ . Though  $F_b$  and  $mg$  are difficult to measure individually,  $F_b/mg$  was obtained from  $V_T$ ,  $w$  and  $\mu$  by Eq. 12. Here  $\mu$  was measured by  $\theta$ .  $\theta$  is sensitive to particle shape.  $\theta$  of dendrite crystals were above  $80^\circ$  and  $\theta$  for melting particles were less than  $50^\circ$ . In Fig. 7, the proportional coefficient between  $V_T$  and  $w$  was about 11, which is  $\sqrt{\mu}$  in Fig. 10 without  $F_b$  and equivalent to  $\theta$  of  $85^\circ$ . Thus  $\mu$  from observed repose angle was suitable to Eq. 10 for dendrite crystals and broad branches. For other particles,  $F_b$  is not negligible and  $V_T$  becomes larger and data scattered as shown in Fig.12.

For bond-neck strength, Schmidt (1980) examined

a relation between threshold drag forces  $F_c$  to break a bond of ice spheres. Assuming  $F_v$  is same as  $F_c$  and  $C=1$  in Eq. 1, a ratio of  $x/R$  is estimated from the relation of Schmidt(1980); when  $V_0$  is 5 m/s, 10 m/s, 15 m/s,  $F_c$  is 2.3 Pa, 9.0 Pa, 20 Pa and  $x/R$  can be 0.03, 0.05, 0.07 respectively. Though it is difficult to observe  $x/R$  in the field experiments, this ratio of  $x/R$  obtained above seems to be appropriate for the particle size and neck radius of dendrite crystal.

## 6. Concluding remarks

The following results were obtained from the measurements of threshold wind velocity  $V_T$ , terminal wind velocity  $w$  and repose angle  $\theta$  for snow samples obtained from a natural snow surface.

- 1)  $V_T$  values for dendrite crystals, dendrite crystals with rime and broad branches were 3–6 m/s, 6–13 m/s and 5–12 m/s, respectively.
- 2)  $V_T$  for the dendrite crystals subsequent to snowfall was small, i.e. 3–6 m/s; however, it increased to 10–15 m/s in a short period of 1–3 days, accompanying a change in particle shape.
- 3) The  $w$  values for the dendrite crystals, dendrite crystals with rime, broad branches and melting particles were 0.4–0.7 m/s, 0.5–1.2 m/s, 0.6–0.8 m/s and 0.6–1.4 m/s, respectively.
- 4) In the case of the dendrite crystals,  $V_T$  tends to be proportional to  $w$ . The  $V_T/w$  ratio of the other particles was larger than that of the dendrite crystals, which

is explained by the existence of a bonding force.

- 5) The repose angle  $\theta$  was measured as 80–90° for the dendrite crystals and 25–50° for the melting particles.
- 6) The normalized bonding force  $F_b/mg$  between the particles was greater than 50 for the melting particles, while it was negligible for the dendrite crystals.
- 7) In order to apply the  $V_T$  values obtained in this study to natural snow drifting, they should be multiplied by 1.3.

## References

- Budd, W. F., Dingle, W. R. J. and Radok, U. (1966): The Byrd Snow Drift Project Outline and Basic Results (Part II; S5, S6), Antarctic Res. Ser. **9**, 71–134.
- Radok, U. (1977): Snow Drift. *Journal of Glaciology*, **19**, 123–138.
- Satoh, K., Takahashi, S. and Tanifuji, T. (2003): Threshold wind velocity for snow particle movement and its variation with snow surface condition. *Journal of The Japanese Society of Snow and Ice*, **65**, 189–196. (in Japanese)
- Schmidt, R. A., Threshold wind-speeds and elastic impact in snow transport. *Journal of Glaciology*, **26** (94), 453–467, 1980.
- Shiotani, M. and Arai, H. (1953): A short note on the snow storm. Second National Congress for Applied Mechanics, Science Council of Japan.
- Takahashi, S. (1985): Characteristics of Drifting snow at Mizuho Station, Antarctica. *Annals of Glaciology*, **6**, 71–75.
- Takeuchi, M., Ishimoto, K., and Nohara, T. (1975): A Study of Drift Snow Transport. *Journal of The Japanese Society of Snow and Ice*, **37**, 114–121. (in Japanese)